Article

JOURNAL OF COMPOSITE MATERIALS

Journal of Composite Materials
2018, Vol. 52(10) 1331–1338

DOI: 10.1177/0021998317723694
journals.sagepub.com/home/jcm
SAGE

Heat transport in epoxy and polyester carbonyl iron microcomposites: The effect of concentration and temperature

NW Pech-May[1,2], C Vales-Pinzon[3], A Vega-Flick[1], A Oleaga[2], A Salazar[2], JM Yanez-Limon[4] and JJ Alvarado-Gil[1]

Abstract

Temperature dependence of the thermal diffusivity in composites of epoxy and polyester resins, loaded with carbonyl iron particles, has been studied using the photopyroelectric technique. Increments of eight and 2.5 times the thermal conductivity of the polymers are obtained, as the volume concentration of microparticles is increased from 0% to 40% for epoxy and from 0% to 20% for polyester matrices, respectively. Additionally, the thermal diffusivity falls systematically as the temperature is increased from 270 to 400 K; the effect is more pronounced for high concentration of microparticles in epoxy composites. The glass transition of the composites is explored by implementing a numerical differentiation algorithm. In order to explain the consequences of the loading of the composites on the thermal conductivity, a modified Lewis-Nielsen model, which includes the presence of crowded regions in the samples, is used to study heat transfer in a wide range of particle concentrations.

Keywords

Polymeric composites, thermal diffusivity, photopyroelectric calorimetry, Lewis-Nielsen model

Introduction

Many devices required for micro-electronic applications demand specific physical properties of materials, such as good electrical and thermal conductivities.[1,2] Moreover, lightweight is also a mandatory requirement, which limits the usage of most metals. Accordingly, the possibility of satisfying all of these requirements by using polymeric composites loaded with metallic micro- and nanoparticles has been widely studied.[3,4] In particular, several electronic devices (mobile phones, network areas, etc.) operate in the low-frequency range microwave radiation, increasing the problem of electromagnetic interference.[4–6] In order to minimize or completely eliminate this problem, metallic magnetic particles have been used as electromagnetic absorbers in polymeric matrices.[7] Several studies have shown that carbonyl-iron powder (CIP) acts as a good electromagnetic wave absorber in polymers.[6,8] Moreover, it has been shown that when carbon nanotubes are added to the fillers, the shielding of the composites to electromagnetic waves is enhanced.[4] However, aside from microwave shielding and good electrical conductivity, thermal properties are also indispensable for the use of composites in real applications. Enhancement of the thermal conductivity in polymers has been achieved using several kinds of metallic particles. For example, it has been reported that adding copper (25% in volume) and nickel (40% in volume) to an epoxy resin matrix can enhance 7.9 and five times the thermal conductivity of the resin, respectively.[1]

[1]Applied Physics Department, CINVESTAV-Unidad Mérida, Mexico
[2]Departamento de Física Aplicada I, Escuela Superior de Ingeniería de Bilbao, Universidad del País Vasco, Spain
[3]Facultad de Ingeniería-UADY, Av. Industrias no Contaminantes por Periférico Norte, Mexico
[4]Centro de Investigación y de Estudios Avanzados del IPN-Unidad Querétaro, Mexico

Corresponding author:
NW Pech-May, Centro de Investigacion y de Estudios Avanzados Unidad Merida, Carretera Antigua a Progreso km 6, Cordemex, Merida, 97310, Mexico.
Email: nelson.pechmay@gmail.com

Similarly, increments of about 5.5 times the thermal conductivity of epoxy resin with 40% volume concentration of CIP has been obtained. Moreover, the alignment of CIP particles using an external magnetic field has been studied as an alternative way to enhance the thermal conductivity of the polymers along a preferred direction. However, it has been shown that the enhancement due to alignment is similar to that of non-aligned particles for high-volume concentrations.[9]

The photopyroelectric (PPE) technique is one of the most sensitive methodologies to retrieve the thermal diffusivity of thin solid samples down to a few hundred microns thickness, since it provides excellent signal-to-noise ratio.[10] Furthermore, even though it is a contact technique, it has been shown to be a good methodology for the characterization of thermal transport properties as a function of temperature. This allows high accuracy identification of phase transitions or critical behavior in most solids.[11–13] The dependence of the thermal diffusivity as a function of the temperature has been studied in several amorphous polymers. In particular, it has been reported that the thermal diffusivity decreases close to the glass transition and this decrease inversely depends on the changes of the specific heat.[14] This shows a close relationship between the results obtained by photothermal techniques and conventional differential scanning calorimetry (DSC), which is usually applied for the identification of the glass transition temperature (T_g).[15,16]

The effective medium approach (EMA) provides good estimation of the effective thermal conductivity in composites with low particle loadings.[17,18] Extensions and generalizations of the EMA have been done in order to include higher particle loadings taking into account the thermal interface resistance between the particles and the matrix, the role of the local arrangement of the particles as well as their orientation and agglomeration.[2,19–21] On the other hand, it is well known that high-volume concentrations have to be used in polymeric composites loaded with microparticles, in order to achieve thermal conductivity values acceptable for real applications in electrical and electronic devices.[22]

In this work, the thermal diffusivity as a function of temperature is studied. The samples consist of epoxy and polyester resins loaded with 2 μm CIP particles at several volume concentrations: 1, 5, 10, 20 and 40% of CIP microparticles in epoxy resin and 1, 5, 10 and 20% of CIP for the polyester resin matrix. The thermal diffusivity, at room temperature, of each sample is determined using the PPE technique. The temperature dependence of the thermal diffusivity of the composites is studied using a PPE calorimeter. The temperature range for these measurements has been chosen in such a way that the glass transition for each specimen is observed. Additionally, a numerical differentiation algorithm based on the total-variation regularization[23–25] is implemented, which allows to identify the T_g of the studied specimens by performing numerical derivatives of the thermal diffusivities as a function of temperature. Finally, a study is performed regarding the thermal conductivity enhancement, at room temperature, of the composite samples as a function of the CIP volume concentration. The specific heat capacities of the epoxy and polyester resins is determined by DSC, which in combination with the measured values of the thermal diffusivity of the samples and using the law of mixtures, allows the calculation of the effective thermal conductivity of the composite samples. The thermal conductivity enhancement achieved is explained using the Lewis-Nielsen model[20,26] with a modification of the form factor in order to take into account crowding effects due to high concentration of particles in our composites.

Experimental

Materials

Polydisperse carbonyl-iron powder HS (BASF) with an average particle diameter of 2 μm, see Figure 1(a), has been used as the filler medium. Two polymeric matrices have been used: polyester resin (RESINMEX MR-227) and epoxy resin embedding medium kit (Sigma Aldrich) consisting of epoxy embedding medium, 2-dodecenylsuccinic anhydride (DDSA), methylnadic anhydride (MNA), 2.4.6-tris dimethylaminomethyl phenol (DPM-30).

Polyester/epoxy – CIP composites preparation

Two types of composites loaded with CIP have been prepared: the first one made with a matrix of polyester resin and the second one with epoxy resin. For the polyester resin composites, CIP microparticles (0, 1, 5, 10 and 20% volume concentration) were added to the polymeric resin and stirred mechanically at 300 r/min

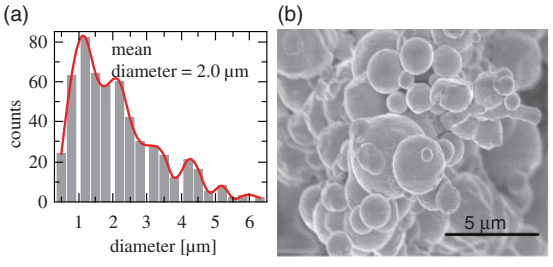

Figure 1. (a) Size dispersion of the particles diameters and (b) SEM image of the carbonyl-iron particles used to make up the composite samples.
SEM: scanning electron microscope.

during 20 min until a homogeneous suspension was obtained. After that, 5% volume concentration of catalyst was added to the mixture and was stirred during the next 2 min. The mixture was cast on a mold allowing the samples to polymerize for 24 h at room temperature. Finally, the sample was post-cured at 80°C for 4 h. The same procedure was used for each volume concentration of CIP.

The epoxy resin matrix is obtained by combining two mixtures. Mixture-A consists of 38% epoxy embedding medium and 62% DDSA (volume concentration) and mixture-B consists of 53% epoxy embedding medium and 47% MNA (volume concentration). Both solutions were stirred for 10 min before being mixed in a 1.15 ratio (A/B) to obtain the epoxy embedding matrix. CIP microparticles (1, 5, 10, 20 and 40% volume concentration) were added to the epoxy matrix and stirred mechanically at 300 r/min during 20 min in order to obtain a homogeneous suspension. Then, 1.5% (volume concentration) of accelerator DPM-30 was added to the mixture and stirred during the next 2 min. The mixture was cast on a mold and polymerized at 80°C for 4 h. The same processes were used for each concentration of CIP. Both kinds of composite samples (polyester- and epoxy-based) were polished to obtain uniform flat samples (1 cm × 1 cm) with a thickness of 300 μm.

Scanning electron microscopy

Figure 1(b) shows a scanning electron microscope (SEM) image of CIP, obtained using a field emission scanning electron microscope (JEOL JSM-7600F) in the back-scattering configuration. Notice the good quality of the spherical shape of the particles. As can be seen from Figure 1(a), the particles diameters are in the range from 1 to 3 μm and the mean diameter is 2 μm.

Photopyroelectric calorimetry

The thermal diffusivity of the composites was studied using a photopyroelectric calorimetry (PPEC), which consists of a $LiTaO_3$ pyroelectric detector (350 μm thick) coated with a Ni-Cr thin layer on each surface, acting as electrodes. A 50-mW laser diode (665 nm, Melles Griot) modulated by a lock-in amplifier (7265 DSP, Signal Recovery) is used as the heating source on the sample surface, which is coated with a 3 -μm graphite layer in order to increase its optical absorption at the exciting wavelength. The PPE signal is collected by the same lock-in amplifier in the electric current mode and saved into a PC for further analysis. A normalization with respect to the frequency response of the bare detector is required in order to take into account the instrumental response. The studied sample is positioned on the top surface of the PPE detector, applying a thin layer of thermal grease (Dow Corning, 304 Heat Sink Compound) between those surfaces, while the back surface of the PPE detector is in contact with a material of similar thermal effusivity (bismuth was used for all measurements), in order to increase the accuracy of the measurements.[10] Both the PPE detector and the studied sample are introduced in a liquid nitrogen cooled cryostat (Optistat-ND, Oxford Instruments) that allows measurements in the temperature range from 77 K to 550 K, at heating–cooling rates varying from 10 to 100 mK per minute, according to requirements.[11,27]

The representation of the natural logarithm of the normalized amplitude $\mathrm{Ln}(|T_n|)$, and the normalized phase Ψ_n, vs $\sqrt{f}$ allows to use the slopes method to identify the thermal diffusivity of the graphite-coated (opaque) samples[11]

$$D = \frac{l^2 \pi}{m^2} \tag{1}$$

where l is the thickness of the sample and m is the slope obtained from $\mathrm{Ln}(|T_n|)$ or Ψ_n vs $\sqrt{f}$. Actually, the mean value of the thermal diffusivity retrieved from amplitude and phase analysis in each measurement is reported.

Figure 2 shows the characteristic behavior of $\mathrm{Ln}(|T_n|)$ and Ψ_n, as a function of the modulation frequency, obtained from a sample of epoxy resin loaded with 40% of CIP particles in volume. For frequencies below 4 Hz, the sample is in the thermally thin regime. For larger frequencies, the sample is in the thermally thick regime $\left(\sqrt{\pi D/f} \ll l\right)$ and the signal is proportional to $\sqrt{f}$. This has been used to determine the thermal diffusivity using the slopes method.[10,11,27] For higher frequencies, the piezoelectric response of the

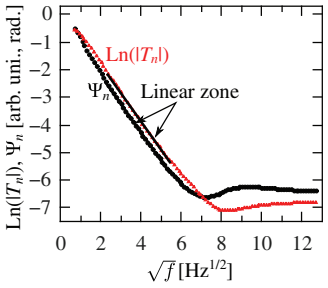

Figure 2. Typical plots of $\mathrm{Ln}(|T_n|)$ and Ψ_n vs $\sqrt{f}$ for a sample of epoxy resin with 40 % CIP in volume. The linear zone of the curves is used to retrieve the thermal diffusivity of the sample. Experimental results for $\mathrm{Ln}(|T_n|)$ are represented by red triangles and black dots are used for Ψ_n, while continuous lines represent the linear fits. CIP: carbonyl iron powder.

detector dominates and therefore it deviates from the linear behavior.[28]

For the temperature-dependent measurements only the evolution of Ψ_n is needed at a fixed frequency in the linear zone.[11,12] Accordingly, the phase difference is defined as $\Delta_0(T) = \Psi_n(T) - \Psi_n(T_{ref})$, where $\Psi_n(T)$ is the normalized phase at the temperature T and $\Psi_n(T_{ref})$ is the normalized phase at room temperature T_{ref}. The thermal diffusivity as a function of the temperature is evaluated with the following expression[11]

$$D(T) = \frac{1}{\left(\frac{1}{\sqrt{D_{ref}}} + \frac{\Delta_0(T)}{l\sqrt{\pi f_0}}\right)^2} \quad (2)$$

where l is the thickness of the sample, f_0 is a reference frequency in the linear zone used for the measurement during the temperature ramp and D_{ref} is the thermal diffusivity of the sample at room temperature.

Results

Thermal diffusivity measurements

Figure 3 shows the thermal diffusivity of epoxy composites and polyester composites as a function of the CIP volume concentration. It is worth mentioning that the thermal diffusivity enhancement is three times for epoxy composites with 20% CIP volume concentration and two times for polyester resin loaded with 20% CIP volume concentration. The uncertainties in the thermal diffusivities are below 5% in all cases and have been estimated after five measurements.

Figure 4 shows the temperature evolution of the thermal diffusivity for epoxy (Figure 4(a)) and polyester (Figure 4(b)) resin samples loaded with different CIP volume concentrations. Measurements were performed in a PPE calorimeter using a temperature ramp from 260 to 415 K for epoxy samples and 230 K to 380 K for polyester samples. The temperature was increased uniformly at a constant rate during 24 h. The modulation frequency of the laser beam was set to 2.37 Hz in order to stay in the linear zone of the model (see Figure 2). Notice that the thermal diffusivity decreases as the temperature rises no matter the concentration of CIP. However, as the concentration of particles increases, the thermal diffusivity is larger in all the temperature range studied. Notice that the rate of change of the thermal diffusivity is not monotone, but it is higher around the T_g. For the polyester composites, the glass transition zone is wider than for the epoxy ones, making it more difficult to identify the T_g.

Glass transition temperature identification

The T_g of polymers is an important parameter for industrial applications. Consequently, alternative methodologies to the well-known DSC have been explored in literature. However, in some cases it is difficult to determine the T_g accurately.[29–31] In particular, the analysis of the temperature dependence of the thermal diffusivity and its slope has been studied for the determination of the glass transition.[14,32] Nevertheless, this approach did not provide acceptable results since the noise involved in the experimental data is highly amplified by finite difference methods, making it almost impossible to determine the numerical derivative. Hence, in this work the total-variation regularization (TVR) method[23,24] is used to obtain the numerical derivative of the thermal diffusivity data shown in Figure 4. This method allows to compute the derivative of a function D_T on $[0, L]$ as the minimizer of the Tikhonov-TV functional[23]

$$F(u) = \alpha TV(u) + \frac{1}{2}||Au - D_T||^2 \quad (3)$$

where $TV(u)$ stands for the total-variation (TV) of u, i.e. it is a regularization term that penalizes irregularity in u, the second summation is a data fidelity term which penalizes discrepancy between Au and D_T. α is a

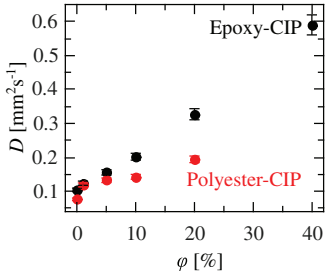

Figure 3. Thermal diffusivity, at room temperature, as a function of CIP volume concentration obtained with the PPE technique. Epoxy-CIP composites are represented by black dots and polyester-CIP by red dots.
CIP: carbonyl iron powder; PPE: photopyroelectric.

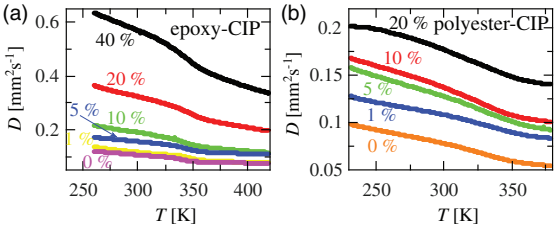

Figure 4. Evolution of the thermal diffusivity as a function of temperature for composite samples of (a) epoxy resin and (b) polyester resin loaded with CIP at several volume concentrations.
CIP: carbonyl iron powder.

regularization parameter which controls the balance between the two terms. Thus, equation (3) yields a regularization scheme for operator equation $Au = D_T$, D_T being the thermal diffusivity as a function of temperature, A the anti-derivative operator and $u = \partial D_T/\partial T$ stands for the derivative of D_T, which is the main interest. It is important to say that the TVR method not only suppresses noise but also allows for the computation of discontinuous derivatives, since it does not suppress jump discontinuities unlike most regularization schemes. The numerical implementation to minimize equation (3) has been done following the gradient descent approach.[24]

The results of u for the different CIP volume concentrations studied are shown in Figure 5 (a and b), for the epoxy- and polyester-based composites, respectively. In most cases, the T_g can be identified, as the minimum of the derivative of the thermal diffusivity with respect to temperature. It is important to mention that only 8 to 12 iterations were necessary to obtain the numerical derivatives and the time consumption was about 20 s for each kind of composite, using a computer with 3 GB RAM memory and 1.3 GHz processor.

Figure 5(c) shows the T_g as a function of the CIP volume concentrations studied. Epoxy-CIP composites are represented by black dots and polyester-CIP composites by red dots. For the latter composites, the derivatives of the thermal diffusivity results in wider Gaussian curves, this is because the glass transition develops over a broader range of temperatures than for the epoxy-CIP composites. It is important to mention that the values obtained for the T_g of the pure polyester (334 K) and pure epoxy (337 K) are in good agreement with previous results in literature[29,31]: 333 K and 335 K, respectively.

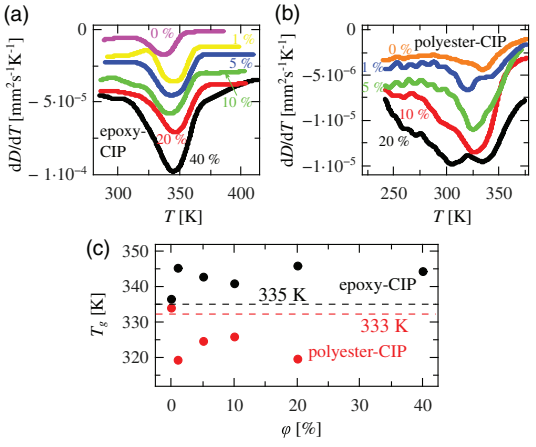

Figure 5. Numerical derivatives of the thermal diffusivities of (a) epoxy composites and (b) polyester composites, as a function of temperature. (c) Glass transition temperatures identified for the studied specimens: epoxy- and polyester-based composites. Dashed lines represent the literature values for pure epoxy and polyester.

Discussion

As a particular case, the effective thermal conductivity K at room temperature of each specimen has been studied, using the well-known relation[33] $K = (\rho C)_p D$, where D is its effective thermal diffusivity and $(\rho C)_p$ its effective volumetric heat capacity obtained according to the law of mixtures.[34,35] The effective thermal conductivity can be written as

$$K = [C_{CIP}\rho_{CIP}\varphi + C_m\rho_m(1-\varphi)]D \qquad (4)$$

φ being the volume concentration of CIP particles. The density of the CIP particles (ρ_{CIP}) is 7.87 gcm^{-3} and ρ_m stands for the density of the polymeric matrix. The density of epoxy and polyester resins is 1.22 gcm^{-3} and 1.16 gcm^{-3}, respectively. These values are provided by the manufacturer. The specific heat capacity of the CIP is 0.45 Jg^{-1}K^{-1}, which is lower than 1.4 Jg^{-1}K^{-1} and 2.1 Jg^{-1}K^{-1} obtained for epoxy and polyester resins, respectively. The specific heat capacities were measured using a differential scanning calorimeter DSC-50 (Mettler-Toledo) employing sapphire as reference for the specific heat capacity identification. In order to guarantee reproducibility on the C_p studied and to avoid possible thermal gradients inside the samples, all studied specimens were 300 μm thick.

Figure 6(a) shows the results of the effective thermal conductivity (at room temperature) for the two kinds of composites studied as a function of CIP volume concentration. The uncertainties were calculated following the error propagation theory.[36] The thermal conductivity for both epoxy and polyester composites increases as the CIP content does. This is in agreement with previous results.[9] Moreover, the thermal conductivity of

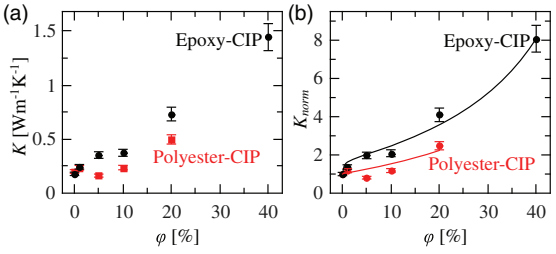

Figure 6. (a) Effective thermal conductivity of epoxy (black dots) and polyester (red dots) composites as a function of the volume concentration of CIP particles. (b) Normalized thermal conductivity (K/K_m) of epoxy-CIP (black dots) and polyester-CIP (red dots) composites. Dots represent the experimental results and continuous lines correspond to the fittings using the Lewis-Nielsen model.
CIP: carbonyl iron powder.

epoxy composites reaches a value of $1.4\,\mathrm{Wm^{-1}\,K^{-1}}$ for the maximum concentration used (40% CIP in volume), which is acceptable for real applications, since the threshold thermal conductivity value is $1.0\,\mathrm{Wm^{-1}\,K^{-1}}$ for heat sinks in electronic devices.[22] However, for the polyester composites at the maximum CIP concentration studied (20% in volume), the thermal conductivity is about $0.5\,\mathrm{Wm^{-1}K^{-1}}$, which is below the mentioned threshold limit. Nevertheless, good increments in the thermal conductivity with respect to the polymeric matrices were obtained for both kinds of composites.

In order to analyze the measured thermal conductivities, the Lewis-Nielsen model[20] has been applied

$$K_{norm} = \frac{1 + AB\varphi}{1 - B\Psi\varphi} \tag{5}$$

where the normalized thermal conductivity $K_{norm} \equiv K/K_m$ is the ratio between the effective thermal conductivity of the polymer composite (K) and the thermal conductivity of the polymer matrix (K_m), the B factor is given by

$$B = \frac{K_p/K_m - 1}{K_p/K_m + A} \tag{6}$$

$$\Psi = 1 + \left(\frac{1 - \varphi_m}{\varphi_m^2}\right)\varphi \tag{7}$$

K_p being the thermal conductivity of the CIP particles and Ψ a function which takes into account the effect of the maximum packing fraction of particles (φ_m) in the thermal conductivity of the composite. In equations (5) and (6), A is referred to as the ''form factor'' and takes into account the shape (aspect ratio) of the particle fillers as well as their orientation with respect to the heat flux. For spherical inclusions, it can take values between 1.5 and 5.5.[37,38] Moreover, when high-volume concentrations are used in the composite samples, interactions between neighboring particles must be taken into account. These interactions can lead to agglomeration of particles that consequently modify the form factor. Lewis and Nielsen considered that these clusters of particles have their own packing fraction $(\varphi_j < \varphi_m)$ composed of the filler particles and part of the matrix trapped inside the agglomerate.[39]

In this work, the form factor is modified by the presence of a low fraction of agglomerates in the composites

$$A = A_0\varphi_a \tag{8}$$

where A_0 is the value of the form factor in the dilute limit (low concentrations). φ_a is referred to as the crowding factor[40,41] and is defined by $\varphi_a = \left(\sum_{j=1}^{M} \varphi_j\right)/\varphi$, where φ_j is the packing fraction of the j-th agglomerate $(\varphi_j \le \varphi_m)$ and M is the number of agglomerate regions in the composite. In the case were there is no agglomeration of particles, $\sum_{j=1}^{M} \varphi_j = \varphi$ and the form factor returns to the dilute limit value A_0, i.e. $\varphi_a = 1$. On the other hand, the maximum agglomeration allowed is obtained for $M = 1$ and $\varphi_1 = \varphi_m$, which establishes the upper limit of the crowding factor $\varphi_a = \varphi_m/\varphi$. This value can be ≥ 1 for any particle volume concentration.

The above definition of the crowding factor implies a strong dependence on the morphology of each composite, thus it would be very difficult to determine an analytical functional form. Accordingly, a simplified effective agglomerate packing fraction φ_c is considered, such that $\varphi_a = f(\varphi_c; \varphi)$. In order to obtain its functional form, an additional restriction is imposed to the crowding factor: it should reach its maximum allowed value asymptotically. All above conditions are satisfied by

$$\varphi_a = 1 + \frac{\varphi_m}{\varphi} - \frac{\varphi_m}{\varphi}\exp\left(-\frac{5\varphi_c}{\varphi_m}\right) \tag{9}$$

where φ_c represents the average packing fraction of all agglomerates present in the composite. This assumption provides accurate results in the dilute limit of agglomerates ($\varphi_c/\varphi_m \ll 1$). In this limit, equation (9) simplifies to a linear form: $\varphi_a \approx 1 + 5\varphi_c/\varphi$.

Figure 6(b) shows the fittings between the thermal conductivity predicted by the Lewis-Nielsen model (continuous lines) with the modified form factor given by equations (8) and (9) and the experimental data obtained for the epoxy-CIP and polyester-CIP composites. There is good agreement between the Lewis-Nielsen model and the experimental results. The thermal conductivity of the CIP particles is $50.2\,\mathrm{Wm^{-1}\,K^{-1}}$,[9,42] while for epoxy and polyester resins it is $0.18\,\mathrm{Wm^{-1}\,K^{-1}}$ and $0.20\,\mathrm{Wm^{-1}\,K^{-1}}$, respectively. These values were obtained from measurements of thermal diffusivity and heat capacity. The maximum packing fraction was set to $\varphi_m = 64\%$ according to literature values.[20,41] Two free parameters A_0 and φ_c have been considered in the fittings. The obtained values are $A_0 = 5.5$, $\varphi_c = 2.9\%$ and $A_0 = 3.6$, $\varphi_c = 0.1\%$ for epoxy-CIP and polyester-CIP composites, respectively. Both form factor values (A_0) are in good agreement with literature[37,38] and the packing fractions φ_c are in the dilute limit, as expected.

It is important to mention that the effective thermal conductivity has been increased eight times at the maximum volume concentration (40%) of CIP particles for epoxy-CIP composites, while 2.5 times for polyester-CIP composites at the maximum volume concentration (20%) of CIP particles. If we consider the same CIP volume concentration (20%), the epoxy composites still show a higher increment in the thermal conductivity

(four times) compared to the polyester composites (2.5 times). On the other hand, the analysis presented on the thermal conductivity at room temperature could be performed at each measured temperature or at those temperatures of interest for practical applications as long as the heat capacity is measured at the same heating or cooling rate than the thermal diffusivity.

Conclusions

The temperature dependence of the thermal diffusivity for epoxy- and polyester-based composites loaded with several volume concentrations of CIP was studied using the PPE technique. It was shown that the T_g could be obtained by measuring the thermal diffusivity as a function of temperature (using small heating rates). The implementation of a total variation regularization method enabled the extraction of the T_g with high accuracy. Additionally, a modification to the Lewis-Nielsen model was proposed that takes into account agglomeration effects of the filler particles. The calculations performed with the modified model are in agreement with the measured thermal conductivities of the composites at room temperature.

Declaration of Conflicting Interests

The author(s) declared no potential conflicts of interest with respect to the research, authorship, and/or publication of this article.

Funding

The author(s) disclosed receipt of the following financial support for the research, authorship, and/or publication of this article: This work has been supported by Gobierno Vasco (IT619-13) by UPV/EHU (UFI 11/55), by Gobierno Vasco (IT906-16) and (KK-2015/00071), by CINVESTAV Unidad Mérida, by the Fund Conacyt-SENER-Energy-Sustainability Grant 207450, within Strategic Project CEMIESol-Cosolpi No. 10 ''Solar Fuels & Industrial Processes'' as well as by Projects 192 ''Fronteras de la ciencia'' and 251882 ''Investigación Científica Básica 2015''.

References

1. Mamunya YP, Davydenko VV, Pissis P, et al. Electrical and thermal conductivity of polymers filled with metal powders. *Eur Polym J* 2002; 38: 1887–1897.
2. Gao L, Zhou X and Ding Y. Effective thermal and electrical conductivity of carbon nanotube composites. *Chem Phys Lett* 2007; 434: 297–300.
3. Qing Y, Zhou W, Luo F, et al. Microwave electromagnetic properties of carbonyl iron particles and Si/C/N nanopowder filled epoxy-silicone coating. *Physica B Condens Matt* 2010; 405: 1181–1184.
4. Qing Y, Zhou W, Luo F, et al. Epoxy-silicone filled with multi-walled carbon nanotubes and carbonyl iron particles as a microwave absorber. *Carbon* 2010; 48: 4074–4080.
5. Lee SE, Choi O and Hahn HT. Microwave properties of graphite nanoplatelet/epoxy composites. *J Appl Phys* 2008; 104: 033705.
6. Kimura S, Kato T, Hyodo T, et al. Electromagnetic wave absorption properties of carbonyl iron-ferrite/PMMA composites fabricated by hybridization method. *J Magnet Magnet Mater* 2007; 312: 181–186.
7. Liu L, Duan Y, Liu S, et al. Microwave absorption properties of one thin sheet employing carbonyl–iron powder and chlorinated polyethylene. *J Magnet Magnet Mater* 2010; 322: 1736–1740.
8. Joseph N and Thomas Sebastian M. Electromagnetic interference shielding nature of PVDF-carbonyl iron composites. *Mater Lett* 2013; 90: 64–67.
9. Medina-Esquivel RA, Zambrano-Arjona MA, Mendez-Gamboa JA, et al. Thermal characterization of composites made up of magnetically aligned carbonyl iron particles in a polyester resin matrix. *J Appl Phys* 2012; 111: 054906.
10. Mercuri F, Marinelli M, Zammit U, et al. Photopyroelectric method. *J Thermal Anal* 1996; 47: 87–92.
11. Salazar A. On the influence of the coupling fluid in photopyroelectric measurements. *Rev Sci Instr* 2003; 74: 825–827.
12. Marinelli M, Mercuri F, Zammit U, et al. Photopyroelectric study of specific heat, thermal conductivity, and thermal diffusivity of Cr_2O_3 at the N'eel transition. *Phys Rev B* 1994; 49: 9523–9532.
13. Zammit U, Paoloni S, Mercuri F, et al. Self consistently calibrated photopyroelectric calorimeter for the high resolution simultaneous absolute measurement of the specific heat and of the thermal conductivity. *AIP Adv* 2012; 2: 012135.
14. Morikawa J, Tan J and Hashimoto T. Study of change in thermal diffusivity of amorphous polymers during glass transition. *Polymer* 1995; 36: 4439–4443.
15. Hutchinson JM and Montserrat S. The application of modulated differential scanning calorimetry to the glass transition of polymers. I. a single-parameter theoretical model and its predictions. *Thermochimica Acta* 1996; 286: 263–296.
16. Pham JQ, Mitchell CA, Bahr JL, et al. Glass transition of polymer/single-walled carbon nanotube composite films. *J Polym Sci B Polym Phys* 2003; 41: 3339–3345.
17. Maxwell JC. *A treatise on electricity and magnetism*. New York: Dover Publications, 1954.
18. Bruggeman DaG. Berechnung verschiedener physikalischer konstanten von heterogenen substanzen. I. dielektrizittskonstanten und leitfhigkeiten der mischkrper aus isotropen substanzen. *Ann Phys* 1935; 416: 636–664.
19. Deng F, Zheng QS, Wang LF, et al. Effects of anisotropy, aspect ratio, and nonstraightness of carbon nanotubes on thermal conductivity of carbon nanotube composites. *Appl Phys Lett* 2007; 90: 021914.
20. Pal R. On the Lewis – Nielsen model for thermal/electrical conductivity of composites. *Compos A Appl Sci Manuf* 2008; 39: 718–726.
21. Pal R. New models for thermal conductivity of particulate composites. *J Reinf Plast Compos* 2007; 26: 643–651.

22. Han Z and Fina A. Thermal conductivity of carbon nanotubes and their polymer nanocomposites: a review. *Progr Polym Sci* 2011; 36: 914–944.
23. Vogel CR. *Computational methods for inverse problems*. Frontiers in Applied Mathematics, Soc for Industrial & Applied Math. Philadelphia: Society for Industrial and Applied Mathematics. ISBN: 978-0-89871-507-1, 2002.
24. Chartrand R. Numerical differentiation of noisy, nonsmooth data, numerical differentiation of noisy, nonsmooth data. *ISRN* 2011; 2011.
25. Rudin LI, Osher S and Fatemi E. Nonlinear total variation based noise removal algorithms. *Physica D Nonlin Phenom* 1992; 60: 259–268.
26. Nielsen LE. The thermal and electrical conductivity of two-phase systems. *Industr Eng Chem Fund* 1974; 13: 17–20.
27. Lizundia E, Oleaga A, Salazar A, et al. Nano- and microstructural effects on thermal properties of poly (l-lactide)/multi-wall carbon nanotube composites. *Polymer* 2012; 53: 2412–2421.
28. Salazar A and Oleaga A. On the piezoelectric contribution to the photopyroelectric signal. *Rev Scientific Instr* 2005; 76: 034901.
29. Michels J, Widmann R, Czaderski C, et al. Glass transition evaluation of commercially available epoxy resins used for civil engineering applications. *Compos B Eng* 2015; 77: 484–493.
30. Liem H, Cabanillas-Gonzalez J, Etchegoin P, et al. Glass transition temperatures of polymer thin films monitored by Raman scattering. *J Phys Condens Matter* 2004; 16: 721.
31. Lucas JC, Borrajo J and Williams RJJ. Cure of unsaturated polyester resins: 1. Heat of copolymerization and glass transition temperature. *Polymer* 1993; 34: 3216–3219.
32. Hashimoto T, Morikawa J, Kurihara T, et al. Frequency dependent thermal diffusivity of polymers by temperature wave analysis. *Thermochimica Acta* 1997; 304–305: 151–156.
33. Carslaw HS and Jaeger JJC. *Conduction of heat in solids*, 2nd ed. Oxford: Clarendon Press, 1986.
34. Salazar A. On thermal diffusivity. *Eur J Phys* 2003; 24: 351.
35. Zhou SQ and Ni R. Measurement of the specific heat capacity of water-based al2o3 nanofluid. *Appl Phys Lett* 2008; 92: 093123.
36. Bevington P and Robinson DK. *Data reduction and error analysis for the physical sciences*, 3rd ed. New York: McGraw-Hill Higher Education, 2002.
37. Mueller S, Llewellin EW and Mader HM. The rheology of suspensions of solid particles. *Proc R Soc A* 2010; 466: 1201–1228.
38. Pabst W, Gregorov E and Berthold C. Particle shape and suspension rheology of short-fiber systems. *J Eur Ceramic Soc* 2006; 26: 149–160.
39. Lewis TB and Nielsen LE. Viscosity of dispersed and aggregated suspensions of spheres. *Trans Soc Rheol* 1968; 12: 421–443.
40. Mooney M. The viscosity of a concentrated suspension of spherical particles. *J Coll Sci* 1951; 6: 162–170.
41. Ordonez-Miranda J, Yang R and Alvarado-Gil JJ. A crowding factor model for the thermal conductivity of particulate composites at non-dilute limit. *J Appl Phys* 2013; 114: 064306.
42. User S. Carbonyl Iron Powder (Fe2(CO)9), (Fe(Co)5), www.reade.com/products/carbonyl-iron-powder-fe2-co-9-fe-co-5 (accessed 31 October 2016).